ELSEVIER

Journal of Photochemistry and Photobiology A: Chemistry 156 (2003) 91–103

Journal of Photochemistry and Photobiology A:Chemistry

www.elsevier.com/locate/jphotochem

Broadening of the fluorescence spectra of hydrocarbons in ethylene-vinyl acetate copolymers and the dynamics of the glass transition

T.D. Martins, S.B. Yamaki, E.A. Prado[1], T.D.Z. Atvars*

Instituto de Química, Caixa Postal 6154, Unicamp, Campinas CEP 13083-970, SP, Brazil

Received 17 June 2002; received in revised form 30 September 2002; accepted 29 October 2002

Abstract

The steady-state fluorescence of two fluorescent condensed aromatic hydrocarbons (anthracene and pyrene) with different fluorescence decay rates (a few nanoseconds and hundreds of nanoseconds, respectively) were employed to investigate the relaxation processes of several random ethylene-co-vinyl acetate copolymers (EVA). Copolymers with various comonomer compositions (EVA-9, EVA-18, EVA-25 and EVA-33) were studied. Data for the EVAs were compared with the same aromatic molecules in low-density polyethylene (LDPE), high-density polyethylene (HDPE) and poly(vinyl acetate) (PVAc) homopolymer models. The fluorescence rate constants were measured by single photon counting at room temperature. The wavelength dependence of the emission spectra (the edge-excitation red-shift (EERS)) were studied at room temperature and at 77 K and the data were interpreted based on the correlation of the differences of decay rates for both molecules and the time correlation of the polymer relaxation processes. The spectral broadenings (full-width at half-maximum (FWHM)) of the fluorescence spectra were studied from 20 to 400 K, which included temperature ranges above and below the glass transition, and these broadenings are compared.

Keywords: Ethylene-co-vinyl acetate copolymers; Spectral broadening; Relaxation processes; Fluorescence spectroscopy; Anthracene and pyrene

1. Introduction

The nature of the glassy state is subjected to several types of studies, some describing this as a true thermodynamic state, some considering this as a non-equilibrium state [1–4]. Independently of the approach to be considered, polymer systems exhibit a very complex micromorphology in the glassy state. The complexity increases substantially if the polymer forms a semi-crystalline solid or if the chemical microstructure is complex, such as with copolymers or branched polymers. In particular, ethylene-co-vinyl acetate (EVA) forms a class of random copolymers whose properties are intermediate between the two homopolymers (low-density polyethylene (LDPE) and poly(vinyl acetate) (PVAc)), depending on the proportion of both comonomers [5–8]. They are semi-crystalline copolymers and the degree of crystallinity depends on the relative amount of the VAc comonomer. The microstructure is composed of an amorphous phase containing ethylene and vinyl acetate units while the crystalline phase is exclusively composed of methylene groups [7–10]. EVA with higher contents of VAc becomes completely amorphous. Nevertheless, it is intriguing that there is no simple relationship between the vinyl acetate content and the polymer relaxation processes in EVA, as shown by the almost constant value of the glass transition temperature for EVA with contents up to 50% VAc [9]. In spite of this, the polarity of the amorphous phase and of the interface changes continuously, as demonstrated both by the change of the intensity of the vibronic bands I and III of the fluorescence emission and by the decay constants of the fluorescence of pyrene [10].

According to the kinetic model for the glass transition [1], the glassy state is characterized by the absence of translational and rotational order. Moreover, several dynamic relaxation processes should take place, depending on the temperature [11]. The time-scale for these processes covers the range from femto to kiloseconds. There are few methods available to probe events with such a broad time-scale. Among them, the optical spectroscopy methodologies may

* Corresponding author. Tel.: +55-19-37883078.
E-mail address: tatvars@iqm.unicamp.br (T.D.Z. Atvars).
[1] Present address: Universidade de Passo Fundo, Campus I, Bairro São José, Passo Fundo CEP 99001-970, Rio Grande do Sul, Brazil.

1010-6030/03/$ – see front matter © 2003 Elsevier Science B.V. All rights reserved.
PII: S1010-6030(02)00401-X

be utilized following several approaches or types of experiments [11–28]. Some of them study the dependence of the fluorescence emission with the excitation wavelength in a rigid or glassy media (edge-excitation red-shift (EERS)); others study the time-resolved fluorescence spectrum and the dependence of the decay rate on the excitation wavelength; and others study the photochemical and non-photochemical hole-burning and photon-eco and the inhomogeneous broadening of the spectra [11–28]. Regardless the type of approach and methodologies, all of them should be useful for comprehension of the mechanisms of motions in the glassy state.

Although the theories supporting the experimental results obtained by optical spectroscopy methods are not straightforward, all of them consider the interaction between the optical center (the guest) and the environment (the host) upon the spectral line shape or emission decay. Moreover, the occurrence of spectral broadening arises as the consequence of these interactions. Indeed, the spectral line shape of a molecule in the gas phase at low pressure is mostly controlled by the excited-state lifetime while the spectrum of the some molecule in a condensed phase is influenced by fluctuations of the local structures of the medium that produce a time-dependent perturbation of the energy levels [11–28]. Thus, when a guest is introduced in the host cavity both the absorption and the emission spectra are broadened because the cavity exhibits a variety of local solvent configurations that are continuously changing at temperatures above 0 K [11–28]. In addition to the broadening, the emission peak might be dependent on the excitation wavelength, if the mobility of the host would be inhibited or if it occurs at a very slow rate. This effect is known the edge-excitation red-shift [11–15].

In an attempt to understand the dynamics of the glass transition and other secondary relaxation processes in polymer systems we assume the hypothesis that the translational and rotational motions are totally frozen in the glassy state and, thus spectral broadening or the EERS effect are both probable. Similar to the EERS effect in solvents, the effect in polymer matrices should be strongly dependent on the temperature and the magnitude of the effect should be enhanced by the increase of the viscosity of the medium [11–15,28]. Thus, we analyzed the full-width at half-maximum (FWHM) and the dynamics of relaxation processes over the temperature range from 20 to 400 K (below and above the glass transition temperature) of several EVA copolymers containing pyrene as fluorescent guest. We compared the profile of the curve of the fluorescence intensity at several temperatures and we associated the slope changes with their polymer relaxation processes [10,29]. We also measured the peak position of the fluorescence band at several temperatures and correlated it with the fluorescence decay of the guest, τ_F, and the relaxation processes of the polymer matrices, τ_R. Two fluorescent molecules (anthracene and pyrene) were employed that exhibit different decay rates (τ_F = 4–5 and 200–400 ns, respectively [10,15]). The dependence of the fluorescence decay rate on excitation wavenumbers was studied at room temperature and was discussed based on the mechanism of inhomogeneous broadening at higher temperatures.

2. Experimental

2.1. Materials

Blown type high-density polyethylene (HDPE) supplied by Polialden and blown type LDPE, additive free, from Poliolefinas (Brazil) were obtained in the form of films. EVA copolymers (Aldrich Chemical Co.) in form of pellets, with different VAc contents, were molded by pressing as previously described [10]. Poly(vinyl acetate) (Aldrich Chemical Co.) was also molded by pressing at 323 K. These films were washed with methanol and *n*-heptane in order to remove impurities, and then were dried in vacuum. Film thicknesses were in the range 60–80 μm. Pyrene (Aldrich Chemical Co., 99%) and anthracene (Carlo Erba) were used as received.

The fluorescent guests were sorbed into the polymer films by swelling the 3 cm × 2 cm strips in 10^{-4} mol l^{-1} in *n*-heptane solution. Then, those films were rinsed thoroughly with methanol to remove the fluorophores on the surfaces and were dried at room temperature in a vacuum oven. The fluorophore concentration was limited to a value where self-absorption/re-emission or excimer emissions are minimized ($\cong 10^{-5}$ mol l^{-1}).

2.2. Methods

Molar mass and molar mass distributions of the PVAc, LDPE, HDPE and EVA copolymers were determined by gel permeation chromatography (GPC) using the protocol previously reported [10].

Vinyl acetate content in all copolymers was determined by thermogravimetric analysis using the mass loss of the first step of the degradation processes [7]. The thermal transitions of the films were determined by differential scanning calorimetry (DSC) (DuPont, model v2.2A 90), calibrated with indium as standard, following the previously established protocol [10]. The melting and the glass transition temperatures as well as the temperatures of the other secondary polymer relaxations were also determined by fluorescence spectroscopy [29].

Steady-state fluorescence spectra of fluorescent probes sorbed in polymer films were measured at room temperature (298 K) and 77 K (liquid nitrogen) using a conventional spectrofluorimeter (Aminco SLM 500). Three wavelengths were chosen for excitation: one coincident with the maximum of the lower energy excitation band and the other two shifted 4–5 nm to the red or to the blue-edge of the excitation peak. The slits of the excitation and emission monochromators were selected in the Aminco spectrofluorimeter to produce ±0.5 nm of spectral resolution.

Steady-state fluorescence measurements at various temperatures were also performed with better resolution (±0.2 nm) using 0.5 m spectrometer (Spex 500 M monochromator) with a photomultiplier tube connected to a lock-in amplifier as described elsewhere [30]. The polymer films inserted between two quartz windows within the cryo-system allowing measurements from 20 to 400 K [30]. The fluorescence spectrum was recorded every 10 K. For the study of the dependence of the fluorescence emission on the temperature, we used only the wavelength coincident with the excitation peak (337 nm for pyrene), selected by a 0.25 m Thermal Jarrell Ash 82-410 monochromator.

Fluorescence decay, at room temperature, was performed by single photon counting (Edinburgh Analytical nF900 system) operating with a pulsed hydrogen lamp. The excitation wavelength coincident with the excitation peak (360 nm for anthracene and 337 nm for pyrene) was the same as those employed with the steady-state spectrofluorimeter. The emission wavelength for the collection of counts was in the fluorescence maximum (402 nm for anthracene and 374 nm for pyrene). Samples were aligned at 45° to the incident radiation and the emission was collected at a right angle from the back face of the polymer film. Samples were sealed in a Vitrocom capillary under vacuum. The instrument response was determined at every measurement using Ludox as scatterer. At least 10^4 counts were collected in the peak channel. Deconvolution was performed by nonlinear least-squares routines using the software supplied by Edinburg.

3. Results and discussion

3.1. Characterization of EVA copolymers

Some physical properties of the polymer and copolymer samples were determined by several techniques and are summarized in Table 1. Although our previous works discuss these data in more detail [10,29], the data depicted in Table 1 show that the HDPE, LDPE and EVA with lower VAc content are semi-crystalline materials and the degree of crystallinity ($w_{cr,DSC}$) decreases with the increase of the VAc content. PVAc is a completely amorphous polymer, with a glass transition temperature ca. $T_g = 305$ K. Using the DSC curves we also determined the melting temperatures and the melting enthalpy (for the semi-crystalline polymer) and the glass transition temperatures (for the amorphous EVAs and PVAc) (Table 1).

In addition to the melting process and the glass transitions, these polymers undergo secondary relaxation processes. These relaxation processes can be determined by several techniques [9,31–48], including the temperature-dependence of the fluorescence intensity [29,49–51]. Fig. 1 shows one example of the dependence the fluorescence spectra on the temperature (range from 20 to 400 K) for pyrene sorbed in HDPE. As we can see, the fluorescence spectra decrease as the temperature increases (Fig. 1a) which can be represented by the decrease of the integrated (over the entire spectral range) and normalized (using the higher intensity emission) fluorescence intensities (Fig. 1b). The decrease of the fluorescence intensity with the increase of temperature is explained by the enhancement of the efficiency of the radiationless processes at higher temperatures, compared with the efficiency of fluorescence emission [15].

The polymer relaxation processes were analyzed by the slope of the curve of the temperature dependence of the fluorescence intensity using the integrated intensity over the entire emission band (from 365 to 440 nm) (Fig. 1b) [29,49–51]. The criterion for defining a relaxation temperature is the change of the slope in the linear I_F versus T plot if and only if the new slope is maintained for the next three values of the integrated intensity. In addition to this, we also considered a confident value for the relaxation temperature

Table 1
Some physical properties of HDPE, LDPE, EVAs and PVAc

	Sample					
	HDPE	LDPE	EVA-9	EVA-18	EVA-33	PVAc
VAc (%)[a]	0	0	9	18	33	100
T_γ (K)[b]	110	110	110–130	110–130	100	80–90
$T_{\gamma 2}$ (K)[b]	160	160	160	–	–	–
T_β (K)	–	–	–	–	180–190[b]	180–190[b]
T_g (K)	220–250[b]	220–250[b]	220[b]	220[b]	230 and 300–310[b]	300–310[b]
	–	–	261[c]	259[c]	257[c]	303[c]
T_α (K)[b]	300	300	270–290	270–290	–	–
T_m (K)	410	383	377	357	337	–
M_n (kg mol^{-1})	15	21	37	21	22	23
M_n/M_w	14.1	16.2	6.0	4.5	2.9	2.9
$w_{cr,DSC}$ (%)[c]	49	40	25	17	–	–

Degree of crystallinity from DSC thermograms ($w_{cr,DSC}$ (%) = $\Delta_m H_{sample}/\Delta_m H_{PE}$; $\Delta_m H_{PE}$: melting enthalpy for 100% crystalline PE [5]).
[a] Weight percentage from TGA.
[b] Values determined by fluorescence spectroscopy [29].
[c] T_g from DSC.

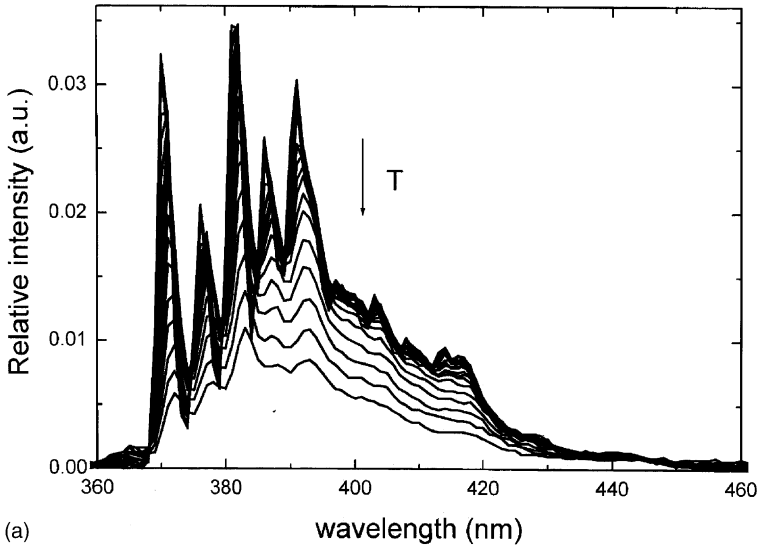

(a)

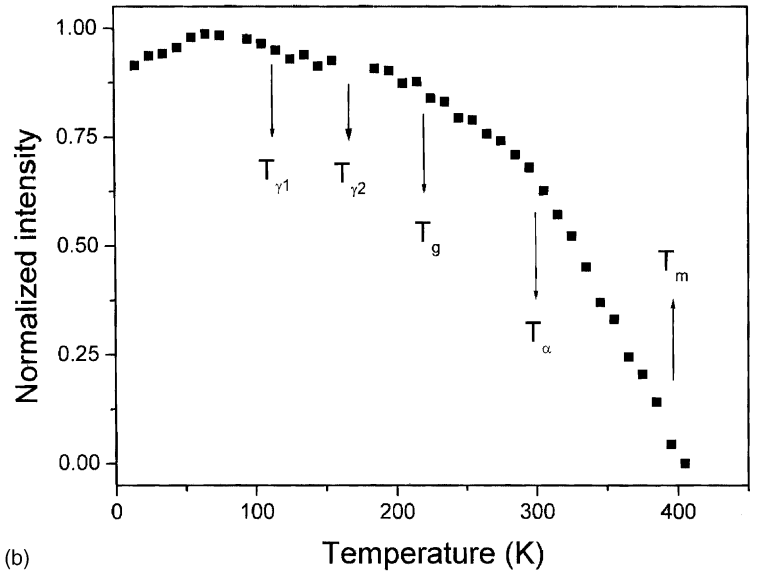

(b)

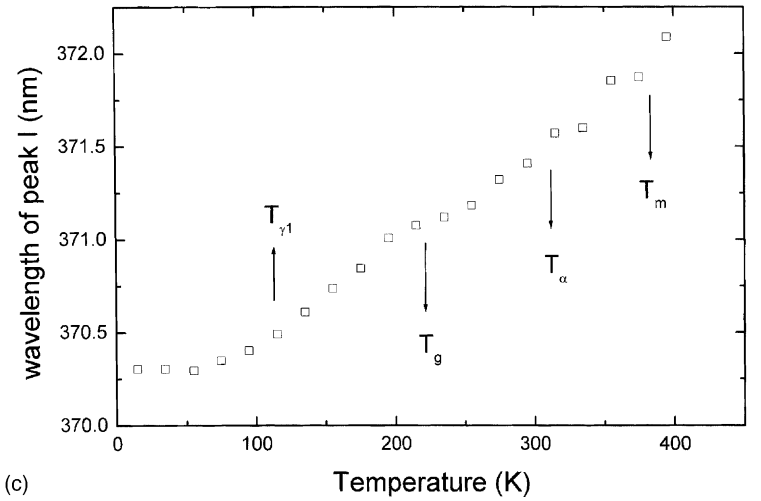

(c)

Fig. 1. (a) Fluorescence spectra of pyrene sorbed in HDPE; (b) integrated intensity of the fluorescence band; (c) wavelength of the vibrational band I (λ_{em} = 372–374 nm). Several temperatures between 15 and 405 K.

when the next three values of the integrated intensities differed by a factor larger than the average distribution of the previous values. These changes occur at well-defined temperatures coincident with the temperature of the relaxation processes of HDPE determined by several other techniques [31–38]. Similar results were obtained for other polymers (LDPE, EVA copolymers and PVAc) and the description and the proposed assignments of these processes are also summarized in Table 1 [29]. It is noteworthy that the slope changes of the fluorescence intensity occur at the same temperatures observed for the polymer relaxation processes determined by other techniques, although some of the assignments are still controversial [9,39–48].

The range of the temperatures of the polymer relaxation processes summarized in Table 1 are: the γ-relaxation processes (temperature range from 110 to 160 K) occur at lower temperatures for PVAc (100 K) than for polyethylenes (LDPE and HDPE) (110 and 160 K) (Table 1). The γ-relaxation involves movements of short segments of the polymer chain as well as movements of the branches and of the end-groups of the chain [9,29,31–48]. The β-relaxation (rotation of VAc groups) occurs in the temperature range of 180–190 K for PVAc and the EVA. The assignment of the β-relaxation processes for polyethylenes is still controversial. Several works reported that the glass transition of polyethylenes occurs from 215 to 250 K while others reported that β-relaxation is occurring in this temperature range [31–39]. Regardless the correct assignment, an unequivocal relaxation process occurs in this temperature range, which we assigned to the glass transition according to the attribution performed for the EVA. This process involves the movements of polymer segments where the fluorescent guest is located, i.e. both the amorphous phase and the interface regions between the crystalline and amorphous phases [29,49–51]. It also involves longer segments of the polymer chain compared with γ-relaxation, inducing a highly efficient fluorescence deactivation. The glass transition of the EVA with the onset temperature at 220 K has also been observed, independent of the VAc content. The glass transition of PVAc is observed at higher temperatures, $T_g = 305$ K. In addition, we also observed α-relaxation occurring from 270 to 300 K for the EVA, LDPE and HDPE, in the order of the increase of the temperature. Since this relaxation involves the presence of a crystalline phase [38] and since the fluorescent guests can not be located inside the crystallites [34,49–51], we attributed this relaxation to the movements of segments located at the interfaces between the amorphous and crystalline regions [29,49–51]. Finally, the melting process of polyethylene segments was observed in the temperature range from 300 to 380 K for some EVA (lower temperatures), LDPE and HDPE (higher temperatures) [29,49–51].

Detailed descriptions of these relaxations were previously reported [29,49–51], which agree with reports using several other techniques [31–48]. Moreover, the relaxation processes determined by fluorescence spectroscopy [29] do not show any correlation among the relaxation processes and the VAc content for the EVAs, in agreement with some reports [9]. Furthermore, the existence of several types of relaxations shows a variety of macromolecular motions with different thermal activation energies, including motions of shorter macromolecular segments at lower temperatures and longer segments at higher temperatures. Each one of these thermally activated movements modifies the relative efficiency of the fluorescence emission reflecting in a decrease of the integrated fluorescence intensity.

3.2. EERS effect and spectral broadening

Three aspects of the fluorescence spectra of anthracene and pyrene in those polymer matrices were analyzed: (i) the dependence of the spectral shift of the fluorescence spectra on the excitation wavelength at both room temperature (above the glass transition for all polymers but PVAc) and at 77 K (all polymers are completely frozen). Three wavelengths were selected: at the peak, at the red-edge and at the blue-edge of the excitation band. (ii) The dependence of the fluorescence decay at room temperature with the sample excited at the peak of the excitation band. (iii) The temperature dependence of the full-width at half maximum in the range from 20 to 400 K. All three types of data are correlated with the mobility of the macromolecular segments forming the cavity where the fluorescence molecules are located [11–28].

We also noted that the peak position of the fluorescence spectra was shifted to a longer wavelength with an increase in temperature (Fig. 1c). Nevertheless, the curve profile exhibited slope changes at the same temperatures attributed to the different types of relaxation processes previously described. Assuming that the peak position reflects the decay from specific Franck–Condon state and that the decays at longer wavelengths originates from more stable (relaxed) excited states, the slope changes are explained by the changes of the solvation layer around the excited molecules that influence the population of the more relaxed fluorescent Franck–Condon states.

A simplified model for describing the relaxation process of the Franck–Condon states is presented in Fig. 2. If the solvation layer is completely immobilized during the excitation, the emission results from the non-relaxed Franck–Condon state ($h\upsilon_F$ in Fig. 2). However, if the solvation layer is able to relax during the lifetime of the excited state, the emission will be changed to lower wavelengths and the decay originates from the relaxed Franck–Condon state ($h\upsilon_{F(F')}$ in Fig. 2). If the relaxation process of the Franck–Condon states is a continuous or a two-level process is still controversial [11–28].

Moreover, based on this model, we consider that the medium below 100 K is completely frozen with the emission occurring from the non-relaxed Franck–Condon states, while the emission at room temperature results from the more relaxed state and is shifted to the red.

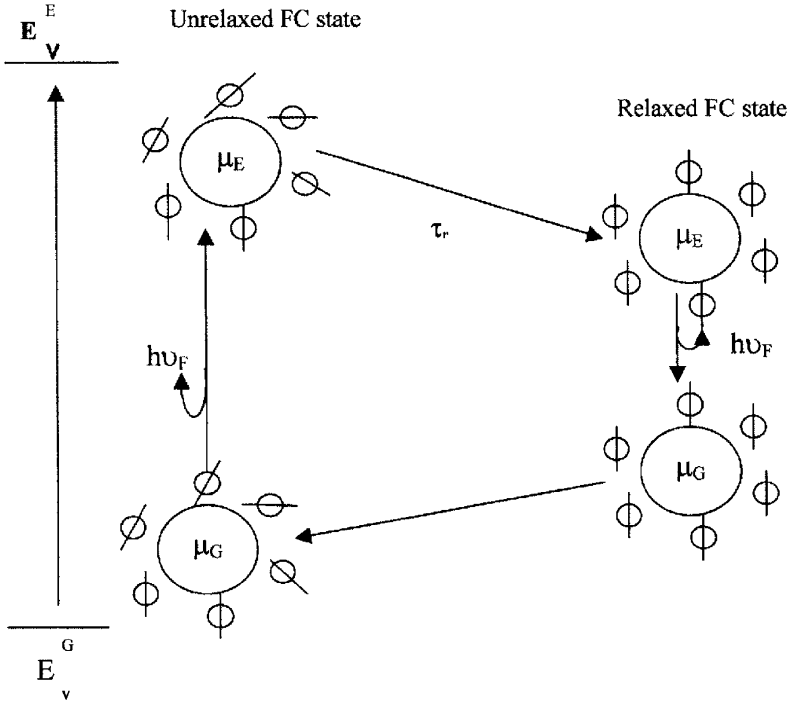

Fig. 2. Scheme for the fluorescence emission from the Franck–Condon states and the relaxation processes of the solvent. E_v^E and E_v^G are the vibronic energy of the excited (E) or ground (G) Franck–Condon (FC) states; μ_E and μ_G are the dipole moments for the molecules in the excited (E) or ground (G) FC states; τ_r is the relaxation time of the solvation layer; $h\upsilon_{F(F')}$ are the energy transition for the fluorescence from the non-relaxed and relaxed FC states; circles are the cartoons for the orientation of the dipole moment of the solvent molecule.

Fig. 3 shows one example of the steady-state excitation and fluorescence spectra using three excitation wavelengths for anthracene (355, 360 and 365 nm) and for pyrene (333, 337 and 341 nm) in EVA-9, at room temperature and at 77 K. The excitation spectra were collected at the fluorescence peak (402 nm for anthracene and 374 nm for pyrene). Similar spectra were also collected for both molecules in the other polymers (not shown). From Fig. 3a and c we note that the peaks of the fluorescence band, at room temperature, were independent of the excitation wavelengths. However, there is a small red-shift of the florescence spectrum at 77 K if the excitation occurs at the red-edge of the excitation band (365 and 341 nm for anthracene and pyrene, respectively) (Fig. 3b and d). In conclusion, the red-shift of the emission spectra for molecules excited at the red-edge of the absorption/excitation band in the frozen matrices demonstrated the presence of the EERS effect.

As is well known, the EERS effect results from the inability of the solvation layer to undergo a relaxation processes around the exited molecule at lower temperatures [11–28]. Consequently, the solvation layer around the excited guest was unable to relax during the lifetime of the electronic excited state and thus, the emission results from the non-thermally relaxed Franck–Condon states (Fig. 2). In contrast, at room temperature the EERS effect was not observed for either anthracene (faster decay rate) or for pyrene (slower decay rate), indicating a decay from the relaxed Franck–Condon state.

Thus, we assume that, although at room temperature all polymer matrices form a solid state host and that in some cases they are semi-crystalline materials (HDPE, LDPE, EVA-9, 18 and probably EVA-33), the cavity where the fluorophores are located relaxes faster than the decay rate of anthracene, which suggests that the cavity is softer than a completely crystalline matrix. This is additional evidence that these guests are not included in the crystalline phase of the host, as is also observed by the absence of distortion of the patterns of the X-ray diffraction peaks, already reported [34,49–51]. So far, the macromolecular segments forming the walls of the cavity where the molecule is located behave, at room temperature, as a sink for a partial dissipation of the energy of the excited molecule. Thus, all molecules decay from a relaxed Franck–Condon state, independent of the excitation wavelength (Fig. 2) [11–28].

Regardless of the origin of the inhomogeneous broadening in a polymer matrix, it should differ from that in the solid crystalline state: a crystalline phase is a more ordered system and a more rigid medium than the amorphous phase of a semi-crystalline polymer. On the other hand, the segments of the chains in the amorphous phase can undergo movement around the guest related to its polymer relaxation processes. At room temperature, all polymers (HDPE, LDPE and EVAs) but PVAc are above the glass transition temperature and the polymer chains should also display long distance movements [3,5]. It was established long ago that the mobility represented by the intrinsic macroscopic

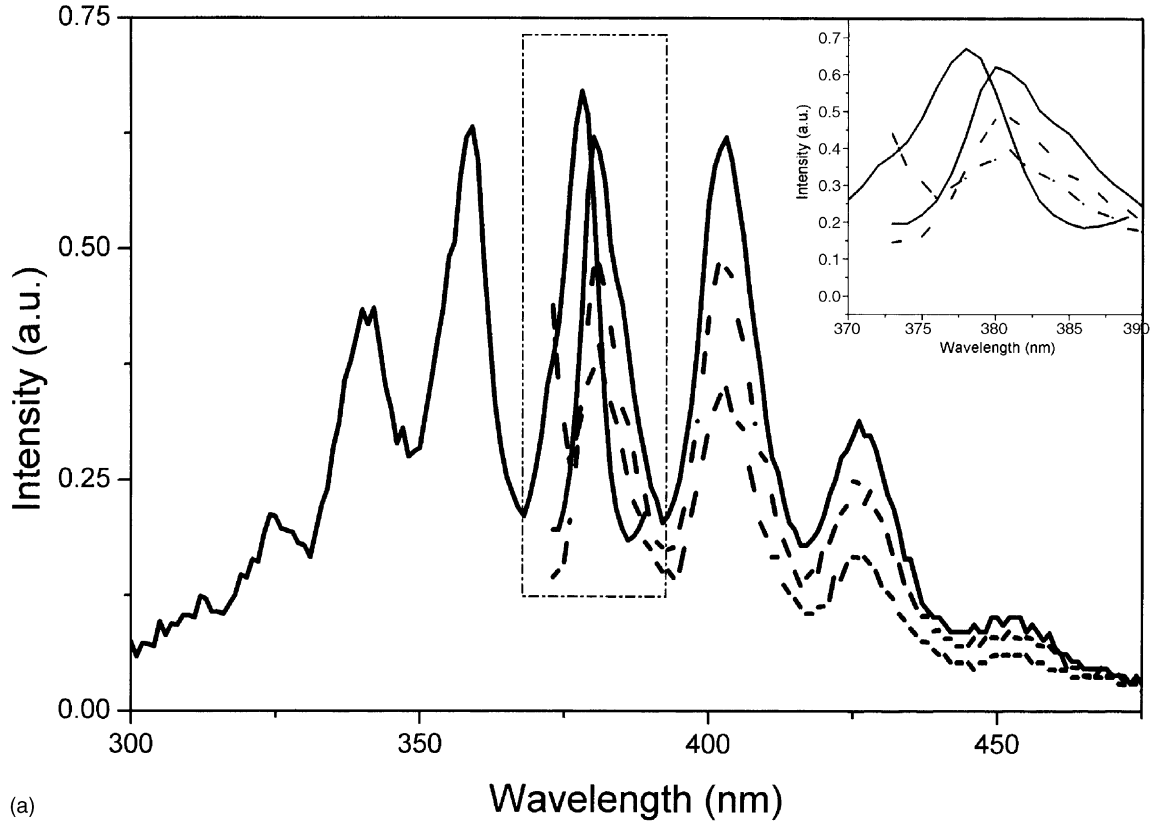

(a)

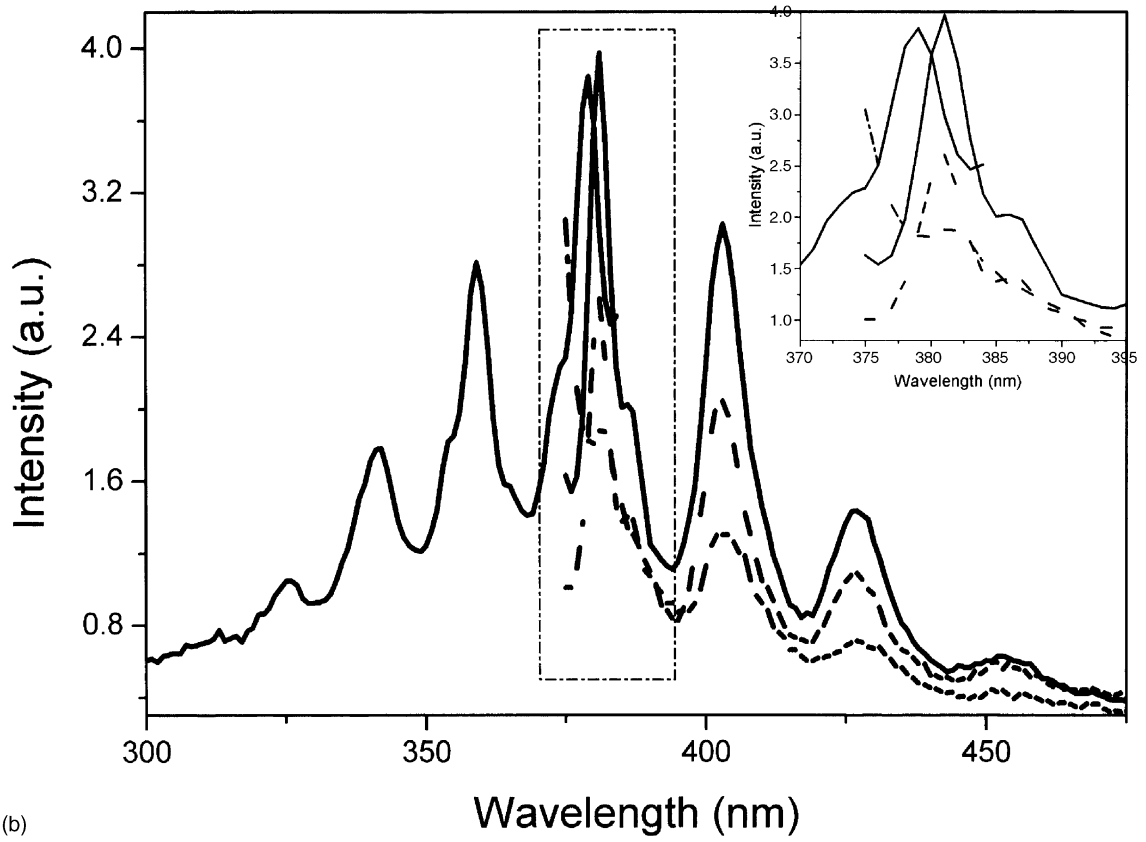

(b)

Fig. 3. Excitation and fluorescence spectra of: anthracene (a, b) and pyrene (c, d) in EVA-9, at room temperature (a, c) and 77 K (b, d). λ_{exc}: (–·–·–) 355 nm, (—) 360 nm and (– – –) 365 nm for anthracene; (–·–·–) 333 nm, (—) 337 nm and (– – –) 341 nm for pyrene.

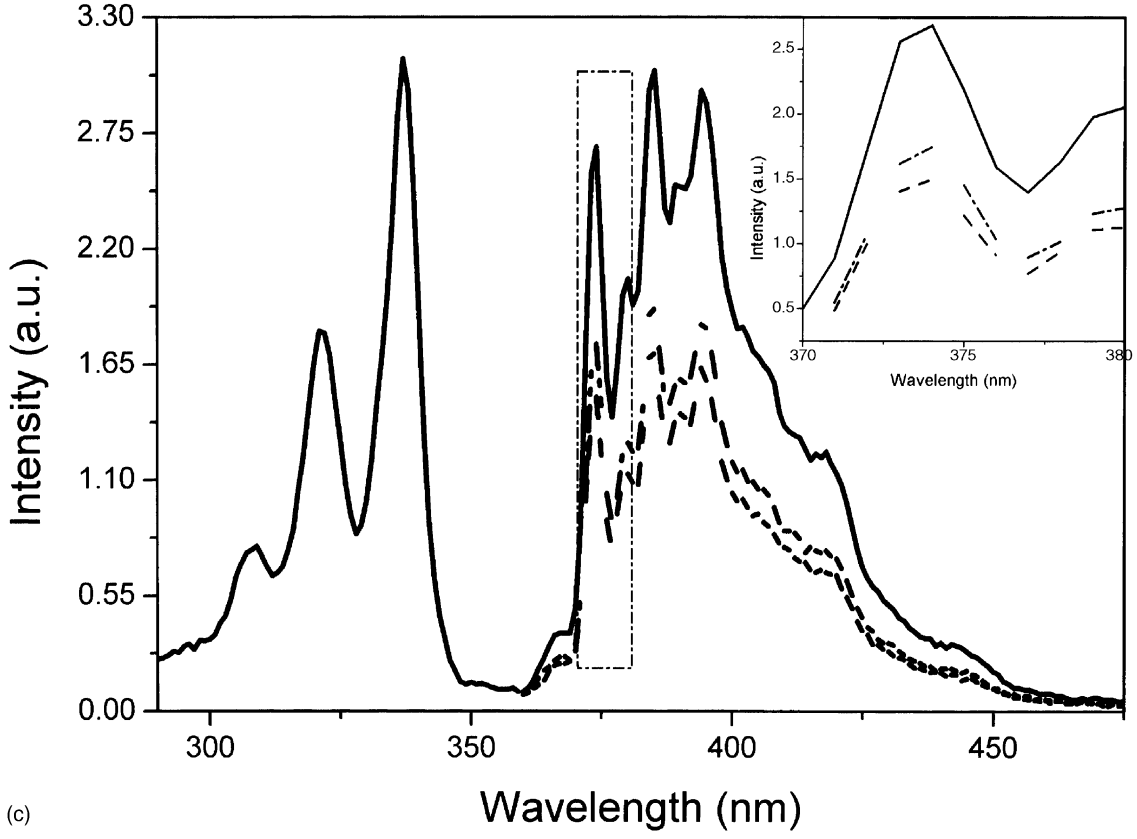

(c)

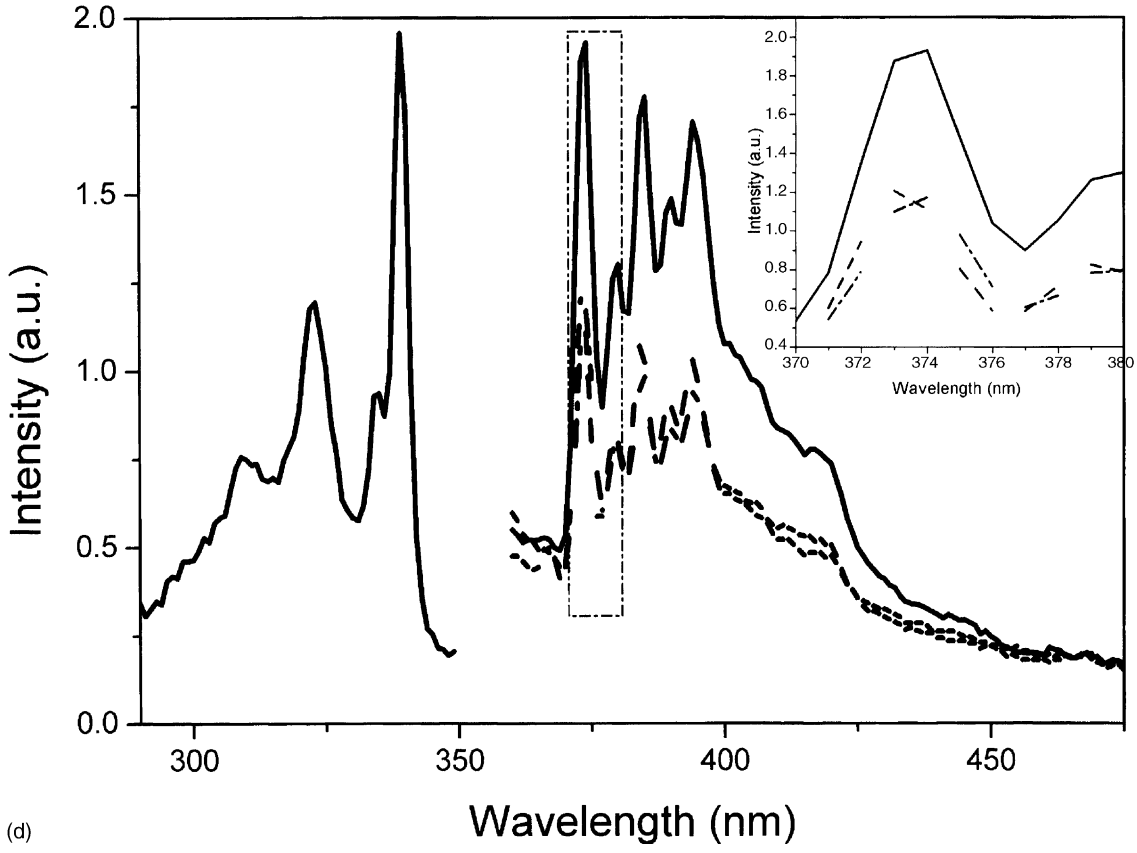

(d)

Fig. 3. (*Continued*).

viscosity or time correlation for rotational and translational relaxation of the medium impacts on the fluorescence intensity [11–28]. In consequence, when the temperature decreased or the solution is very viscous, the fluorescence peak is blue-shifted stepwise and both the fluorescence peak and the fluorescence decay exhibit an excitation wavelength dependence (EERS effect). These effects resulted from the slower dipolar re-orientation of the solvation layer around the molecule during the lifetime of the electronic excited state (Fig. 2). Thus, the emission occurs from an unrelaxed Franck–Condon state and before the relaxation of the solvation layer around the molecule. In contrast, the cavity of the polymer matrix where the guest is located relaxes faster at room temperature than the fluorescence decay rate and, consequently, the steady-state emission was independent of the excitation wavelength.

The analysis of the time correlation between the polymer relaxation and the fluorescence decay was performed by recording the decay curves for both anthracene and pyrene fluorescence at room temperature. Fig. 4 shows examples of these decay curves for both fluorophores in two polymers, the LDPE and the PVAc. Curves for both guests in the other copolymers are similar and are omitted.

The analysis of the decay curves was performed by non-linear least-squares routines minimizing the χ^2 parameters. The experimental curves were fitted by multi-exponential functions (Eq. (1)) using the software supplied by Edinburgh Instruments:

$$I(t) = A_0 + A_1\,e^{-(t/\tau_1)} + A_2\,e^{-(t/\tau_2)} + A_3\,e^{-(t/\tau_3)} \quad (1)$$

where $\tau_1 > \tau_2 > \tau_3$ are decay constants and the A_i are the corresponding pre-exponential terms. Fits were deemed acceptable when $\chi^2 < 1.2$ and no systematic deviations from zero in the corresponding residual plots were apparent. Excluding a very fast decay component from scattered light, the temporal decay curves were fitted with a single-exponential, demonstrated by the acceptability of χ^2 and the corresponding random residual plots (Fig. 4 and Table 2).

From the decay rates depicted in Table 2 we observed that, in general, the fluorescence emissions of both anthracene and pyrene were faster for more polar polymers than for the non-polar polymers although, as expected, the effect was more pronounced for pyrene [10,15]. Data for fluorescence lifetime of pyrene in all polymers follows the expected trend with the polarity. Nevertheless, anthracene shows less

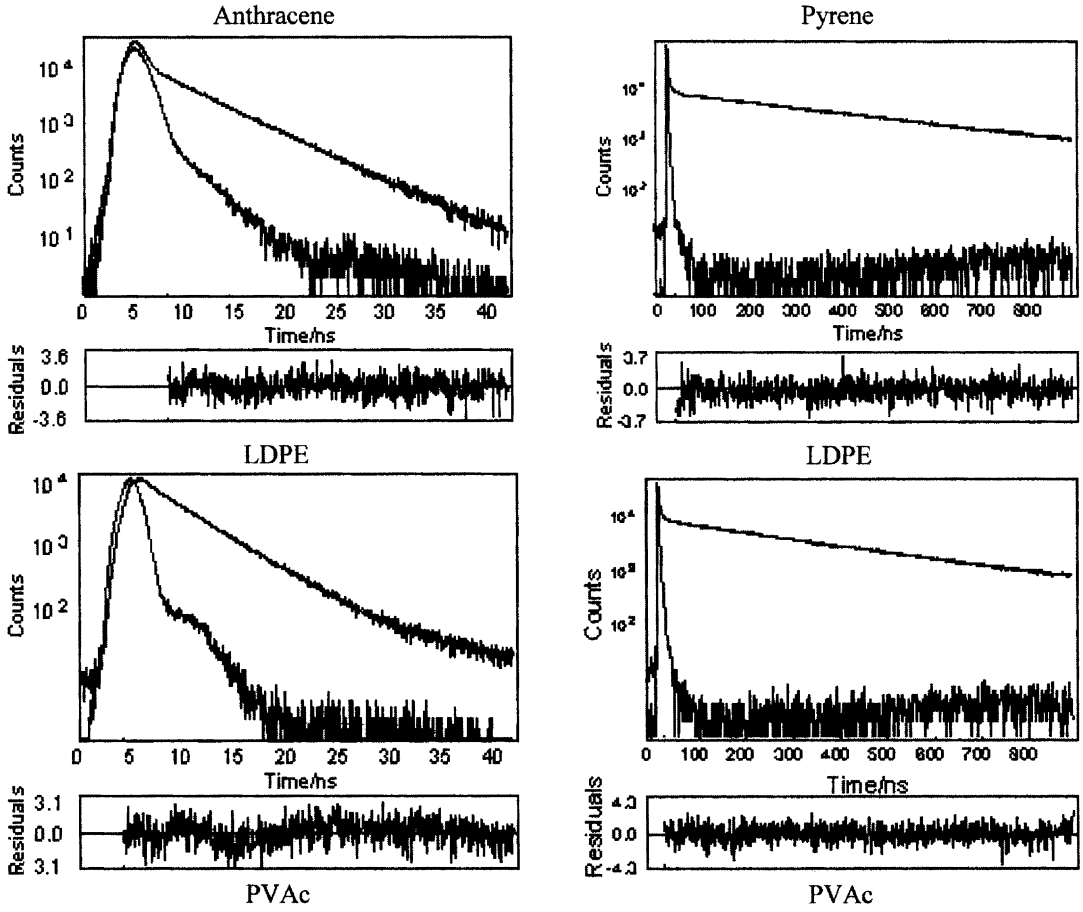

Fig. 4. Fluorescence decay rates for anthracene (λ_{exc} = 360 nm, λ_{em} = 402 nm) and pyrene (λ_{exc} = 337 nm, λ_{em} = 377 nm) in LDPE (top) and PVAc (bottom), at room temperature.

Table 2
Fluorescence decay constants τ_F (ns) and χ^2-values for anthracene (λ_{em} = 402 nm) and pyrene (λ_{em} = 377 nm) excited at the peak of the excitation band at room temperature

	Anthracene		Pyrene	
	τ_F (ns) (λ_{exc} = 360 nm)	χ^2	τ_F (ns) (λ_{exc} = 337 nm)	χ^2
HDPE	4.89 ± 0.01	1.165	–	–
LDPE	4.48 ± 0.01	1.312	400 ± 2	1.047
EVA-9	4.56 ± 0.01	1.29	374 ± 5	1.108
EVA-18	4.0 ± 0.3	1.117	358 ± 3	1.068
EVA-33	4.24 ± 0.01	1.078	346 ± 2	1.002
PVAc	4.23 ± 0.01	1.309	310 ± 3	1.056

sensitivity to the polarity, which means that the decay rates are virtually the same for EVA-18, EVA-33 and PVAc.

Pyrene exhibits slower fluorescence decay rates (τ_F = 200–400 ns) (see Table 2 for the experimental data) than anthracene (4–5 ns). Assuming that these decays exhibit only a weak dependence on the temperature [15], we assume that the anthracene decays are in the range of few nanoseconds while those for pyrene are in the range of 200–400 ns, independent of the temperature. Therefore, the presence or absence of an EERS effect is controlled by the correlation between the relaxation time, τ_R, (or temperature) of the matrix and the fluorescence decay rate of the guest, τ_F, leading to the conclusion that, above a certain temperature, $\tau_R < \tau_F$, the fluorescence originated from the excited state after complete relaxation of the Franck–Condon states. Furthermore, we can conclude that at 77 K the solvation layer relaxes slower than the slower fluorescence decay $\tau_R \gg \tau_F$ = 200–400 ns.

Considering that at 77 K all of the polymers were below the γ-relaxation temperature ($T < 110$ K), the motions of all small segments of the polymer chains were, below this temperature range, also frozen and thus, the EERS effect takes place. This result agrees with data reported using the hole-burning technique, demonstrating that while the time decay rate of organic guests in organic glasses was in the nanosecond time-scale at very low temperatures, the relaxation time of the host was within the millisecond time-scale under the same conditions [28]. Therefore, under these conditions, the large difference of time-scale for the relaxation processes and the fluorescence decay were responsible for the inhomogeneous broadening of both the absorption and the emission spectra by a static mechanism and by the EERS effect [11–28].

We also measured the fluorescence spectra for both fluorophores in polymer matrices of different polarities, from HDPE to PVAc at room temperature and at 77 K (Fig. 5). Samples were excited at the peak of the excitation band. For anthracene we observed a very small spectral shift with the polarity of the medium predictable by the relationship between the Stokes's shift and the solvent properties. This small solvatochromic effect is a consequence of the small changes of the dipole moments upon excitation [15]. Although the Stokes's shift for anthracene was very small, there was a systematic decrease of the Stokes's shifts with the polarity of the medium from 215 cm^{-1} for EVA-33 to 150 cm^{-1} for LDPE that is explained by the larger values of both the dielectric and the refractive index of PVAc, compared with LDPE [5].

In contrast, the Stokes's shifts between the absorption/excitation and fluorescence spectra of pyrene have not been analyzed because the electronic states involved in both transitions are not the same [15]. Nevertheless, for pyrene there is a remarkable dependence of the fluorescence spectra on the polarity of the medium, as shown by the I_1/I_3 vibrational ratio of the fluorescence spectra (Fig. 5) [10].

We also observed (Fig. 5b and d) that the FWHM values are always broader at room temperature compared with those at low temperatures for the same guest in a specific polymer. Moreover, we noted that the FWHM of the fluorescence emission were smaller and the vibronic structure of both excitation and fluorescence bands were better resolved for molecules in LDPE or HDPE than in PVAc (Fig. 5). Qualitatively the sharper spectra in polyethylenes may be explained by considering that the methylene sequence acts as a quasi-linear hydrocarbon matrix different from PVAc, which has bulky side-groups attached to the polymer chain [13–15,52]. In other words, the zero phonon band and the excited phonons are less coupled for these molecules in polyethylene than in the other polymers. Since the EVAs are random copolymers with some VAc side-groups, we expect that both the size and the shape of the macromolecular segments (the methylene chain) able to produce a quasi-linear solvation of the molecules decrease and, thus, the spectrum should be more inhomogeneously broadened with the increase of VAc content. Similar results using hole-burning techniques have already been reported [11–28].

For a better evaluation of the influence of the rigidity of the medium on the FWHM of the emission spectrum, we performed careful measurements of the fluorescence spectra of pyrene using larger spectral resolution (±0.2 nm) in a wider range of temperature, from 20 to 400 K (Fig. 6) with the excitation wavelength at 337 nm for pyryene. The FWHM of the higher energy vibronic band I of the fluorescence emission was determined for pyrene in all polymers using a Gaussian function for deconvolution from the entire spectrum. Using the best fit we determined the FWHM and plotted this value as a function of temperature (Fig. 6).

The profile of the curve for the FWHM of the vibronic band I versus temperature (Fig. 6) for pyrene in these polymers may be divided into three components with different slopes. From 20 to 110 K, where the systems are completely frozen, the peak position (Fig. 1c) and the FWHM exhibited a weaker dependence with temperature. In this temperature range a smooth stepwise red-shift of the emission band with heating occurred (Fig 1c). Furthermore, as soon as the matrix became more semi-crystalline (lower VAc content in the copolymers) the fluorescence bands became sharper. Using

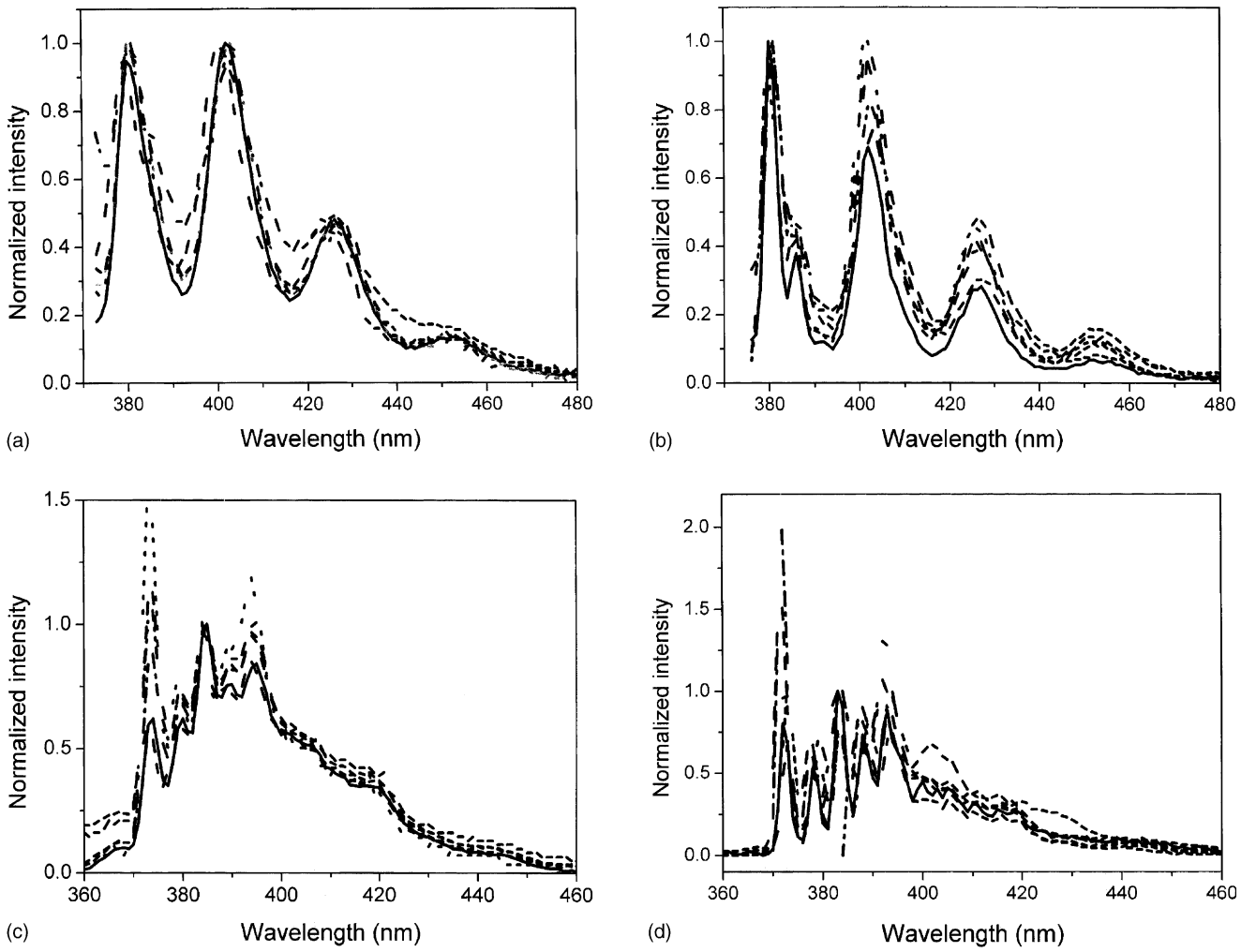

Fig. 5. Normalized fluorescence spectra of anthracene (a and b) and pyrene (c and d) in: (– – –) HDPE, (—) LDPE, (–·–·–) EVA-9, (–··–··–) EVA-18, (—) EVA-33 and (···) PVAc, at room temperature (a and c) and 77 K (b and d).

the curve depicted in Fig. 6, we extrapolated the width for $T \rightarrow 0$ K that is the lifetime-limited origin of the broadening. These values are ca. 119 cm^{-1} for HDPE, 121 cm^{-1} for LDPE, 160 cm^{-1} for EVA-9, 129 cm^{-1} for EVA-18, 161 cm^{-1} for EVA-33 and 139 cm^{-1} for PVAc. It is noteworthy that they are, at least, orders of magnitude broader than the expected value for the homogeneous broadening of a molecule with a decay rate of 200–400 ns, such as pyrene (ca. 5.3×10^{-4} to 10^{-3} cm^{-1} for lifetime-limited values of organic fluorophores with a decay rate on the order of nanoseconds) [14,53]. Nevertheless, they are in agreement with typical half-widths of ca. 100 cm^{-1} observed for organic guests in amorphous environments, which are larger than in crystals (1–20 cm^{-1}) [14].

We also noted in Fig 1c a steeper increase of the peak wavelength with the temperature at $T > 110$ K, although the FHWM still exhibited a weak dependence on temperature (Fig. 6). As discussed previously, at this temperature the onset of the γ-relaxation process occurs.

All these results confirm that, in this temperature range, the molecular emission originates from non-relaxed Franck–Condon states (Fig. 2) and that the polymer relaxation is slower than the slower emission decay rate: $\tau_R > \tau_F = 400$–200 ns. As shown earlier, the relaxation process (γ-relaxation) occurs at 110 K and involves rotation of small segments of the polymer chain located at the amorphous phase and at the interface between the amorphous and crystalline phases of the polymer matrix [49–51]. At the onset of the relaxation process, there is a stepwise red-shift of the spectrum at the same excitation wavelength, which implies that the excess of vibrational energy of the excited-state molecule can be transferred to the medium and be transformed into movements of the small segments of the polymer chain. Since the rigidity of the cavity containing the molecules is still very high, the vertical excitation results in an emission without relaxation of the solvation layer (Fig. 2).

Between 220 and 250 K we observed changes of slope in both the curve for FHWM (Fig. 6) and that related with peak

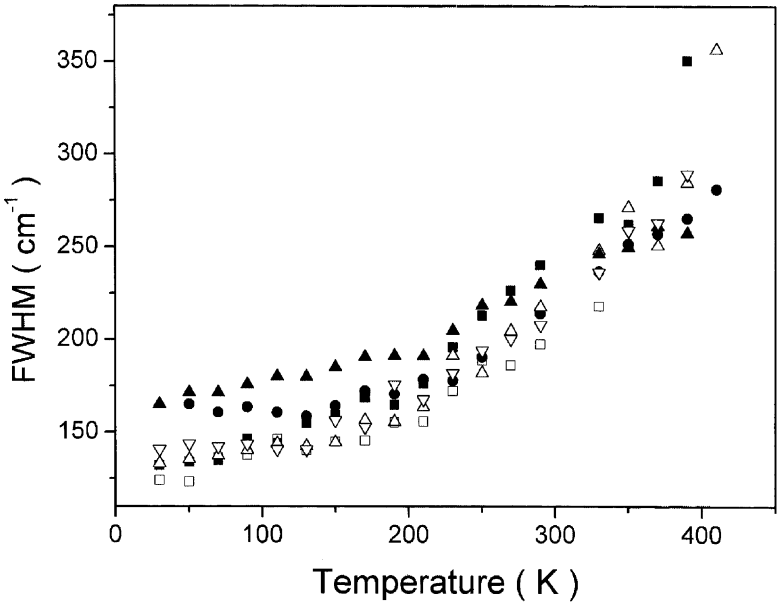

Fig. 6. FWHM (cm^{-1}) of the vibrational band I of the fluorescence spectra of pyrene in: (■) HDPE, (□) LDPE, (●) EVA-9, (△) EVA-18, (▲) EVA-33, and (▽) PVAc at several temperatures (K).

position (Fig. 1c). In addition, in this temperature range, both the λ_{em} values and the FHWM remain almost constant. As previously described, in this temperature range the glass transition for these polymers occurs, with the exception of PVAc. This relaxation changes the surroundings of the guests from a vitreous amorphous material to a viscous-elastic medium. Furthermore, for $T > 250$ K a new stepwise increase of the peak position (Fig. 1c) and a rapid increase of FHWM (Fig. 6) are observed with the increase in temperature. Once the phase transition is completed ($T = 250$ K), the microenvironment where the molecule is located started to exhibit thermal fluctuations involving longer macromolecular segments and the medium starts relaxing faster than the decay rate. It has also been suggested that in a temperature region up to 50 K above the glass transition, the structural relaxation of the liquid still remains relatively slow [28], which should explain the almost constant values of the spectral broadening from 220 to 250 K.

Thus, the time correlation between the polymer relaxation processes and the fluorescence decay is changing at the onset of the glass transition temperature, from a regime where $\tau_R \gg \tau_F$ below T_g to $\tau_R \cong \tau_F$ at T_g. Two mechanisms influencing the spectral broadening of a fluorophore in a solid matrix have been suggested [28]: (1) Below the glass transition, the only possible mechanism of the broadening results from the phonon coupling of the vibronic states of the guest and those of the matrix. (2) Above the glass transition, the vibronic states of the guests are coupled with the structural coordinates of the host, whose mobility determines the macroscopic fluidity of the system [28]. As a consequence, the structural relaxation at the glass transition on the same time-scale as that of the emission spectra produces an additional broadening of the spectrum that was also observed by photochemical hole-burning experiments [28].

4. Conclusions

Inhomogeneous broadening of the fluorescence emission of anthracene and pyrene sorbed in three types of EVA copolymers were compared with the results with two types of HDPE and LDPE and with PVAc. The inhomogeneous broadening of the fluorescence spectra of two guests (anthracene and pyrene) were analyzed from 30 to 400 K and the data were correlated with the polymer relaxation processes.

We observed that the broadening was strongly enhanced for temperatures above the glass transition, demonstrating that there was a time correlation between the relative efficiencies of the fluorescence decay of the guest in a polymer matrix and the relaxation processes of the host.

We also showed that the mechanism of the inhomogeneous broadening changes with the temperature. A time correlation between the polymer relaxation and the fluorescence, $\tau_R \gg \tau_F$, is observed at the lower temperatures, below the glass transition temperature of the medium and under these conditions, the EERS effect should take place.

Using two fluorescent guests (anthracene and pyrene) with very different fluorescence decay rates, we showed that the polymer relaxation processes of the host occurred with a rate slower than hundreds of nanoseconds (the decay rate of pyrene) at low temperatures. Under these conditions, we assumed that the mechanism for the inhomogeneous broadening should be static, i.e. the decay occurs without relaxation

of the polymer cavity. Above the glass transition, where the relaxation processes become faster than a few nanoseconds (the decay rate of anthracene), more remarkable changes of the fluorescence intensity and of the spectral broadening occurred. These results were explained by the structural mechanism of the inhomogeneous broadening that occurs above the glass transition temperature [53]. This remarkable change of the spectral properties above the glass transition suggests that the dynamics of this process strongly influence the mechanism of inhomogeneous broadening.

Acknowledgements

T.D.Z.A. thanks FAPESP and CNPq for financial support. S.B.Y., T.D.M. and T.D.Z.A. acknowledge fellowships from FAPESP and CNPq. E.A.P. acknowledges a fellowship from CAPES/PICD-UPF. The authors also thank Prof. Carol Collins for useful discussions.

References

[1] W. Kauzmann, Chem. Rev. 43 (1948) 219.
[2] J.H. Gibbs, E.A. DiMarzio, J. Chem. Phys. 28 (1958) 373.
[3] G.B. McKenna, in: G. Allen, J.C. Bevington (Eds.), Comprehensive Polymer Science, vol. 2, Pergamon Press, Oxford, 1989, p. 311 (and references herein).
[4] S.B. Yamaki, A.G. Pedroso, T.D.Z. Atvars, Quím. Nova 25 (2002) 330.
[5] H.F. Mark, N.M. Bibales, C.G. Overberger, G. Menses (Eds.), Encyclopedia of Polymer Science and Engineering, 2nd ed., Wiley/Interscience, New York, 1986, p. 6.
[6] S.A. Kumar, S. Thomas, M.G. Kumaran, Polymer 38 (1997) 4629.
[7] W.W. Zaho, X.G. Zhong, L. Yu, Y.F. Zhang, J.Z. Sun, Polymer 35 (1994) 3348.
[8] R.L. McEvoy, S. Kause, P. Wu, Polymer 39 (1998) 5223.
[9] G. Dlubek, Th. Lüpke, J. Stejny, A. Alam, M. Arnold, Macromolecules 33 (2000) 990.
[10] E.A. Prado, S.B. Yamaki, T.D.Z. Atvars, O.E. Zimerman, R.G. Weiss, J. Phys. Chem. B 104 (2000) 5905.
[11] L.R. Narasimhan, K.A. Littau, D.W. Pack, Y.S. Bai, A. Elschner, M.D. Fayer, Chem. Rev. 90 (1990) 439.
[12] G.R. Fleming, M. Chao, Annu. Chem. Phys. Rev. 47 (1996) 109.
[13] S. Volker, Annu. Chem. Phys. Rev. 40 (1989) 499.
[14] A.B. Meyer, Annu. Chem. Phys. Rev. 49 (1998) 267.
[15] J.R. Lackowicz, Principles of Fluorescence Spectroscopy, 2nd ed., Kluwer Academic Publishers, New York, 1999.
[16] N. Agnon, J. Phys. Chem. 94 (1990) 2959.
[17] M.V. Bondar, O.V. Przhonska, Y.A. Tikhonov, J. Phys. Chem. 96 (1992) 10831.
[18] E. Leontideis, U.W. Suter, M. Schutz, H.-P. Luthi, A. Renn, U.P. Wild, J. Am. Chem. Soc. 117 (1995) 7493.
[19] M.J.E. Morgenthaler, K. Yoshihara, S.R. Meech, J. Chem. Soc., Faraday Trans. 92 (1996) 629.
[20] I.V. Litvinyuk, J. Phys. Chem. 101 (1997) 813.
[21] R. Nakamura, A. Ishizumi, J. Watanabe, J. Nakahara, J. Lumin. 76 (1998) 571.
[22] P. Geissinger, B.E. Kohler, S.G. Kulikov, V. Terpougov, J. Phys. Chem. 108 (1988) 1821.
[23] A.S. Ladokhin, J. Fluorescence 9 (1999) 1.
[24] L.W. Molenkamp, D.A. Wiersma, J. Chem. Phys. 83 (1985) 1.
[25] R.F. Loring, Y.J. Yan, S. Mukamel, J. Chem. Phys. 87 (1987) 5840.
[26] M. Maroncelli, G.R. Fleming, J. Chem. Phys. 86 (1987) 6221.
[27] S. Kinoshita, N. Nishi, J. Chem. Phys. 89 (1988) 6612.
[28] J. Yu, M. Berg, J. Chem. Phys. 96 (1992) 8741.
[29] S.B. Yamaki, E. A Prado, T.D.Z. Atvars, Eur. Polym. J. 38 (2002) 1811.
[30] T.D.Z. Atvars, M. Talhavini, Quím. Nova 18 (1995) 298.
[31] M. Kakizaki, T. Kakudate, T. Hideshima, J. Polym. Sci. B: Polym. Phys. Ed. 23 (1985) 809.
[32] B. Wunderlich, The basis of thermal analysis, in: E.A. Turi (Ed.), Thermal Characterization of Polymeric Materials, Academic Press, Orlando, 1981, p. 172.
[33] G.T. Davies, R.K. Eby, J. Appl. Phys. 44 (1973) 4274.
[34] Y.T. Jang, D. Parikh, P.H. Phillips, J. Polym. Sci. 23 (1985) 2483.
[35] P.J. Hendra, C. Passangham, S.A. Jones, Eur. Polym. J. 27 (1991) 127.
[36] M. Glotin, R. Domszy, L. Mandelkern, J. Polym. Sci. B: Polym. Phys. Ed. 21 (1983) 285.
[37] R.F. Boyer, J. Polym. Sci.: Polym. Symp. 50 (1975) 189.
[38] Y. Ohta, H. Yasuda, J. Polym. Sci. B: Polym. Phys. 32 (1994) 2241.
[39] L. Woo, M.T.K. Ling, S.P. Westphal, Thermochim. Acta 243 (1994) 147.
[40] L.E. Nielsen, J. Polym. Sci. 42 (1960) 357.
[41] G.D. Smith, F. Liu, R.W. Devereaux, R.H. Boyd, Macromolecules 25 (1992) 703.
[42] M. Brogly, M. Nardin, J. Schultz, J. Appl. Polym. Sci. 64 (1997) 1903.
[43] D. Dibbern-Brunelli, T.D.Z. Atvars, J. Appl. Polym. Sci. 55 (1995) 889.
[44] S. Yagikara, S. Takeishi, J. Chem. Phys. 77 (1982) 6259.
[45] R. Nozaki, S. Mashimo, J. Chem. Phys. 87 (1987) 2271.
[46] S. Schrader, A. Schonhals, Prog. Colloid Polym. Sci. 80 (1989) 93.
[47] S.S.N. Murthy, J. Chem. Phys. 92 (1990) 2684.
[48] B. Golding, J.E. Graebner, W.H. Haemmerle, Phys. Rev. Lett. 44 (1980) 899.
[49] M. Talhavini, T.D.Z. Atvars, O. Schurr, R.G. Weiss, Polymer 39 (1998) 3221.
[50] M.R. Vigil, J. Bravo, T.D.Z. Atvars, J. Baselga, Macromolecules 30 (1997) 4871.
[51] M. Talhavini, T.D.Z. Atvars, C. Cui, R.G. Weiss, Polymer 37 (1996) 4365.
[52] L. Coltro, D. Dibbern-Brunelli, C.A. Elias, M. Talhavini, M.G. de Oliveira, T.D.Z. Atvars, J. Braz. Chem. Soc. 6 (1995) 127.
[53] H.P.H. Thijssen, S. Völker, J. Chem. Phys. 85 (1986) 785.